# Interplay between optical and electrical properties of nanostructured surfaces in crystalline silicon solar cells

*Amna Safdar* [₸] *, Yue Wang* [‡]*, Christopher Reardon* [‡]*, Juntao Li* [ǁ]*, Guilherme S. de Arruda*[†]*, Augusto Martins*[†]*, Emiliano R. Martins* [†]*and Thomas F. Krauss* [‡]

[₸] School of Chemical and Material Engineering, National University of Sciences and Technology H-12, Islamabad, Islamabad Capital Territory 44000, Pakistan

[‡]Department of Physics, University of York, York, YO10 5DD UK

[†]Sao Carlos School of Engineering, Department of Electrical and Computer

Engineering, University of Sao Paulo, Sao Carlos SP 13566590, Brazil

[ǁ]State Key Laboratory of Optoelectronic Materials and Technologies, School of Physics, Sun Yat-sen University, Guangzhou 510275, China

Email: amna.safdar@scme.nust.edu.pk

KEYWORDS Light trapping, silicon, nanophotonics, nanostructures, solar cell

**ABSTRACT** Light trapping has now been recognised as an essential element of highly-efficient solar cells. A large number of sophisticated nanostructures have been developed and optically characterised, many of which have been aimed at thin film silicon technology. It is still an open question whether such nanostructures are beneficial for thick devices, however, especially since highly efficient solar cells employ >100 $\mu$m thick absorber materials and wet etched micron-sized pyramids for light trapping. Here, we study and compare the optical and electrical performances of binary quasi-random nanostructures with pyramidal structures to address this question. We show that, while simulations indicate that pyramids have better optical performance, the best overall performance observed experimentally was achieved with binary nanostructures. We found that the experimental short circuit current for a solar cell patterned with a quasirandom nanostructure is 3.2 mA/cm$^2$ higher than the current observed with pyramids. We attribute this higher current to a better balance between optical performance and surface recombination achieved by the binary nanostructures. This result indicates that binary nanostructures may be beneficial even for thick solar cells.

The integration of light trapping structures into silicon solar devices is essential for improving the efficiency because light trapping allows the capture of photons that might otherwise be lost, especially at the red end of the spectrum. As a result, all high efficiency silicon solar cell designs

demonstrated to date employ light trapping structures that typically consist of wet etched pyramids[1] , inverted pyramids [2], [3] or honeycomb[4], [5] structures.

As these pyramidal features are typically larger than the wavelength of sunlight, they are not applicable to thin film devices that may have an active layer thickness of only a few microns or less. Therefore, various high-index nanoscale structures have been introduced for thin film solar cells in order to manipulate the in-coupling and trapping of light at the subwavelength scale while maintaining high light trapping efficiency. Nanophotonic morphologies such as nanowires[6], inverted nanopyramids[7], quasi-random nanostructures [8], nanocones [9], inverted nanocones [10] and nanospikes[11] that can control and enhance light absorption fall into this category. These diffractive nanostructures have been designed and studied in the wave optics regime. Their impact on the electrical properties is not yet fully understood, on account of the difficulty of fabricating complete nanostructured thin film solar cells. A common assumption regarding these nanostructures is that they are more suitable for thin film devices than for bulk cells [12]–[16]. Therefore, very few light trapping nanostructures have been implemented and characterised in real devices, and we are not aware of any comparison including electrical measurements in real thick solar cells between light trapping binary nanostructures and the standard pyramidal structures. Such a comparison is important for addressing the following two questions: 1 – is the optical performance of binary nanostructures comparable to that of pyramids, especially in thick solar cells? 2 – is the electrical performance of binary nanostructures better or worse than that of pyramids? This second question is generally overlooked but is particularly important because smaller feature sizes result in smaller surface area for recombination, thus offering a route for improving the electrical properties of silicon solar cells. Hence, there is a need to conduct such a comparison and to understand whether light trapping nanostructures can enhance solar cell performance even for thick silicon devices.

Clearly, nanostructures have two different functions in silicon devices; the first one is light trapping and the second is antireflection (AR). “Light trapping” generally refers to the fact that light is scattered into the absorber with a corresponding increase in pathlength, while “antireflection” only deals with reflection and transmission at the interface, and it does not ask what happens to the light once it has entered the material. Clearly, both functions are distinct. For example, black silicon [17] is a well-known example of a nanostructure that improves antireflection, but it is not necessarily effective for light trapping purposes. For example, Oh et al. have reported an interdigitated back contact (IBC) device with plasma nano-textured black silicon that achieved 18.2% efficiency [18], the good performance being attributed to the AR property of black silicon. Sevin et al. [19] have further improved this result by minimising surface recombination through a conformal alumina coating and they report 22.1% efficiency for a black silicon IBC device. Despite these successes, it is noteworthy that all high-performance cells such as the passivated emitter with rear locally diffused (PERL) cells (25%) [20] and the heterojunction with intrinsic thin layer (HIT) cell (25.6%) [21] employ pyramid-shaped light trapping structures. Hence, the obvious question is whether nanostructures have a role to play even in high efficiency solar cells. In order to address this question, we have investigated nanostructures that have been optimised for light trapping in thin film devices, have improved their antireflection property by applying a standard AR coating and have then applied them to thick silicon solar cells.

We choose quasirandom (QR) nanostructures as our exemplar because they have already demonstrated superior light trapping properties for thin film solar cells [8], [22], [23]. Using numerical simulations, we begin by identifying general optical properties by comparing the

absorption of QR binary nanostructures with two different classes of pyramidal structures. We find that, while high aspect ratios benefit anti-reflection properties, lower aspect ratios benefit light scattering. The question of which structure is best, however, cannot be answered with optical simulations alone, as they do not include the effects of charge carrier recombination. Attempting to answer this important question, we fabricated QRs and random pyramids on top of 180 $\mu$m solar cells. These random pyramidal structures, whose optical performance has been shown to be comparable to the inverted pyramids [24], are formed spontaneously by wet etching in an alkaline solution. Surprisingly, we found that the short-circuit current of the QR structures is about 3.2 mA/cm$^2$ higher than that of the pyramidal structures, thus indicating that nanostructures can be advantageous even in the domain of thick devices.

Figure 1 shows the calculated transmission and absorption of light on a 180 $\mu$m silicon layer, using three different patterns. Figure 1a shows a schematic of the three patterns, consisting of: a 1.8 $\mu$m QR structure using 8 pixels[22], a random distribution of high aspect ratio pyramids (HARP) and a random distribution of low aspect ratio pyramids (LARP). The random pyramids are simulated using supercells of 2 $\mu$m. The aspect ratios of the pyramids are chosen as upper and lower bounds of the typical values obtained experimentally by wet-etching. Transmission, reflection and absorption were calculated using the Rigorous Coupled Wave Analysis [25]. For the structures considered in this manuscript, we found that convergence is reached with less than 450 plane-waves. The tapering of the HARP and LARP structures were modelled in the RCWA using 30 layers.

Figure 1a shows the setup used in all simulations. The difference between the simulations was the type of surface employed on top of silicon, which we indicate as "ARC surface" in Figure 1a. These surfaces are: the HARP, the LARP, the quasi-random or just planar silicon. Figure 1b shows the absorption (solid lines) and transmission (dashed lines) of the QR (blue), – HARP (red) and LARP (green) structures. Notice that the transmission and absorption curves coincide up to about 950 nm. This means that all light injected into the silicon layer is absorbed for wavelengths shorter than ~ 950 nm. Therefore, in a 180 $\mu$m thick silicon layer, scattering is only important in the 950 – 1200 nm wavelength range, whereas the AR effect is predominant at shorter wavelengths.

Inspection of Figure 1b shows that the structure producing the best AR effect is the HARP. This is expected as the high aspect ratio produces a smoother graded effective index transition between air and silicon. On the other hand, it is surprising that the QR has a better AR effect than the LARP in the range between 600 – 1000 nm: since the QR is a binary structure, there is no gradual transition of effective index as in the LARP. Nevertheless, favourable thin-film interference can lead to better transmission in the QR than in the LARP in this spectral window.

In order to quantify the effect of scattering, Figure 1c shows the percentage of transmitted photons that are absorbed. Especially in the spectral region of 900 – 1100 nm, light has to propagate distances larger than the film thickness, thereby requiring scattering and trapping for optimum absorption. The percentage of transmitted photons that are actually absorbed (i.e., the ratio between absorption and transmission) is indicative of the role of light trapping: the higher this percentage, the better is the light trapping afforded by the structures. As Figure 1c shows, the best light trapping performance is achieved by the LARP structures. This positive effect, however, is compensated by the LARP poor AR performance. Indeed, as can be seen in Figure 1b, the absorption of the LARP is lower than the absorption of the HARP up to about 1030 nm, after which they become very similar.

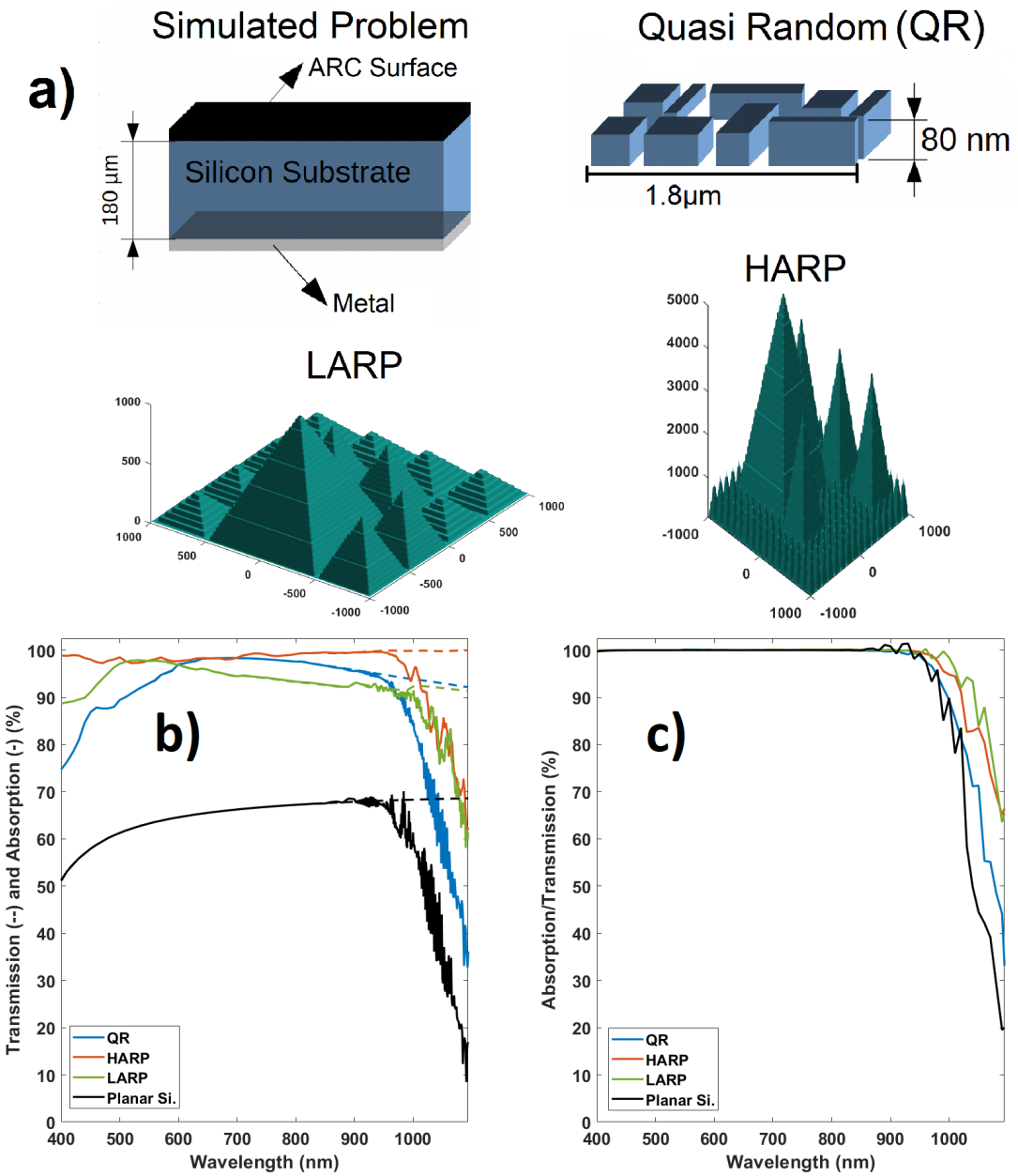


Figure 1 a) schematics of the three investigated structures. b) Absorption (solid lines) and Transmission (dashed lines) of the QR (blue), HARP (red) and LARP (yellow). c) Percentage of transmitted photons that are actually absorbed.

Table 1. Integrated solar photon absorption (ISPA) of the three investigated structures.

| | Quasi Random | HARP | LARP |
|---|---|---|---|
| ISPA | 77.9% | 82.8% | 79.4% |
| ISPT | 94.1% | 98.9% | 93.7% |

The optical performance is best quantified by the integrated solar photon absorption (ISPA), defined as the percentage of absorbed solar photons in the spectral range where silicon absorbs. As shown in Table 1, the ISPAs are 77.9%, 82.8% and 79.4% for the QR, HARP and LARP, respectively. As a reference, we also show the integrated solar photon transmission (ISPT), which is 94.1%, 98.9% and 93.7% for the QR, HARP and LARP, respectively.

The results shown in Figure 1 confirm the general understanding that pyramidal structures are better than binary nanostructures to maximize the absorption in thick silicon solar cells. The suitability of a given structure, however, cannot be determined solely by considering its absorption, since what ultimately matters is the generated photocurrent. In this context, the surface area of the structures is expected to play an important role, as the larger the surface area, the larger the surface recombination rate. [26] [27] The HARP, having the largest surface area, is therefore expected to induce the largest surface recombination rate and the binary QR is expected to induce the lowest surface recombination rate. Therefore, there is a trade-off between optical and electrical performance: higher aspect ratios improve the optical performance but tend to deteriorate the charge collection efficiency. Consequently, it is still an open question which structure is best.

Attempting to answer this question, we fabricated silicon solar cells patterned with nanostructured QR and with pyramids. We used (180 ± 2) $\mu$m thick n-type float zone (FZ) wafers with a resistivity in the range of 1 - 20 ohm.cm and <100> ± 0.5° oriented planes (Siltronix, [France]). Wafers were first sonicated with acetone and isopropanol (IPA) followed by standard RCA cleaning. The p-type emitter was formed by boron diffusion using a boron nitride (BN) solid source (Saint Gobain, p-type) at 975 °C for 40 minutes to achieve a sheet resistance of 50 Ω /□. The boron silicate glass (BSG) that forms during the junction formation was removed with dilute hydrofluoric acid (HF) cleaning. The n-type diffusion process was similarly performed with a phosphorous solid source (Saint Gobain, n-type) on the back side of the wafer at 1000 °C for 20 minutes, resulting in a sheet resistance of 150 Ω /□. The doping processes were followed by thermal oxidation at 850 °C for surface passivation. Another silicon dioxide ($SiO_2$) layer of 80 nm thickness was deposited as an anti-reflection coating using plasma sputtering. Finally, aluminium contacts were deposited by thermal evaporation.

The QR structures were first defined in ebeam resist (CSAR-62-AR-P 6200.09 ALLRESIST GmbH) using electron beam lithography (Voyager, Raith GmbH). The details of the QR structure design are provided in the SI. After exposure, the samples were developed in Xylene at room temperature for 2 minutes. For the dry etched structures, reactive ion etching was used ($CHF_3$:$SF_6$, 14.5 sccm:12.5 sccm, 50 seconds, 80 nm etch depth). Wet etching was performed with 25 wt.% tetramethylammonium hydroxide (TMAH) at 65 °C for 7, 10 and 13 minutes resulting in etch depths of 50 nm, 70 nm and 100 nm, respectively. The backside of the device was protected by a thermally grown (850°C, 30 minutes) $SiO_2$ mask. For the pyramidal structure, the same alkaline etch solution (25 wt.% TMAH) was used but at higher temperature of 85° C for 30 minutes, and without a mask. Since the (100) planes etch much faster, this results in spontaneously forming pyramids with (111) planes as facets.

The surface topography was characterised by scanning electron microscopy (JEOL FE-SEM 7800) and by atomic force microscopy (Bruker BioScope Resolve AFM). The sheet resistance ($R_{sheet}$) was measured using a four-point probe JANDEL (Model RM3-AR) on the polished front and back diffused surfaces before texturing the nanostructures. The current-voltage (IV) measurements were performed with a halogen lamp and the setup was calibrated by using a reference solar cell of known efficiency. A monochromator (Omni-λ150, Gilden Photonics) was used to define the spectrum over a wavelength range of 350 - 1100 nm with an integrating sphere (Labsphere 3P-GPS-040-SF). The $SiO_2$ layer thickness was measured using a spectroscopic ellipsometer. For the external quantum efficiency measurements, the illumination spot size was kept at a fixed size of (5x2) mm, which is smaller than the device size of (2x2) cm to avoid reflection from the contact bars.

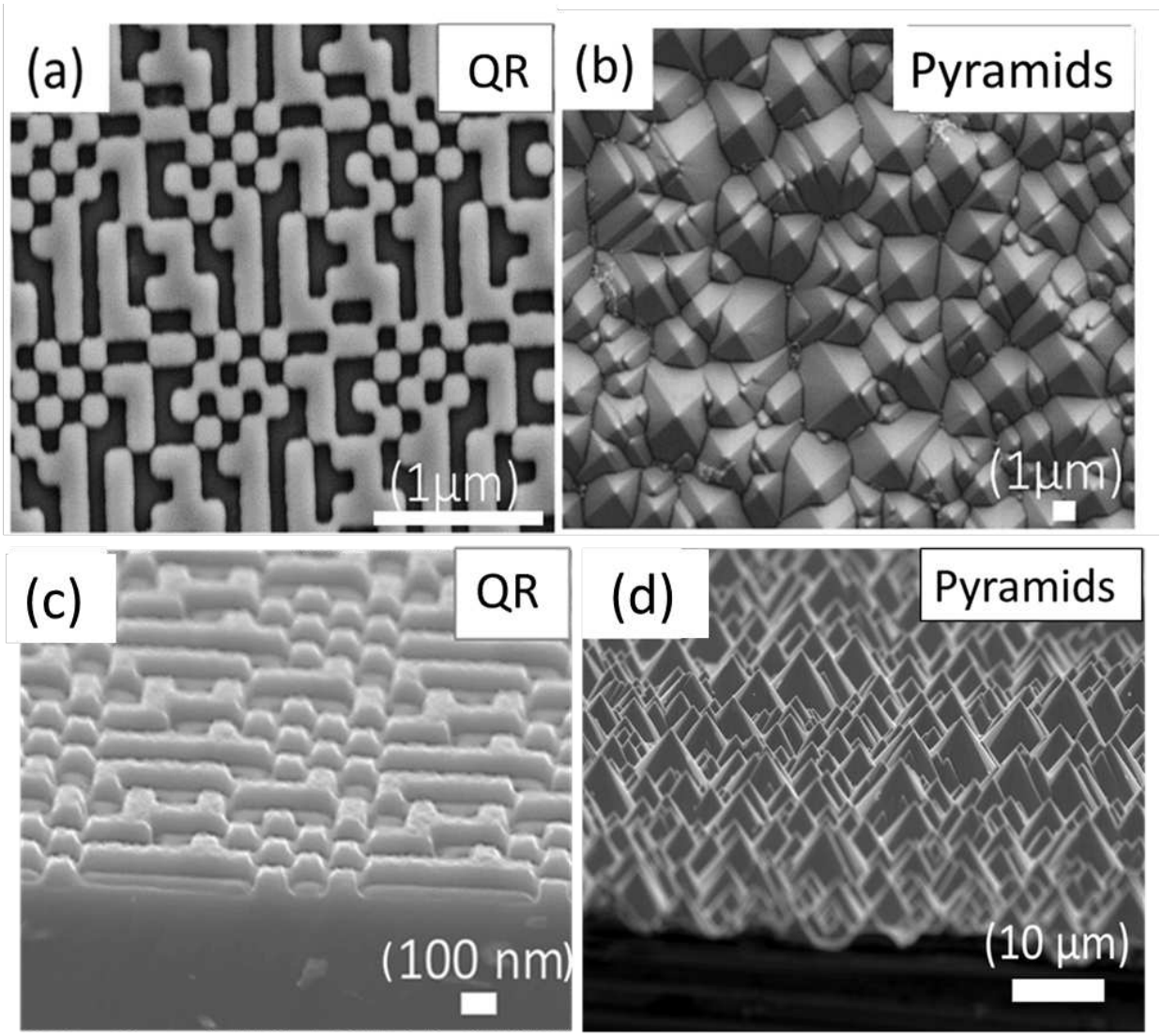


**Figure 2.** Surface micrographs of (a) dry etched quasirandom (QR); QR and (b) wet etched pyramids; (c) Perspective view of QR; (d) pyramids to allow a comparison of different etch depths and feature sizes.

Scanning electron micrographs of the two types of structures are shown in Figure 2a, 2b (top view) and Figure 2c, 2d (perspective view). For a comparison of the different dry etched structures,

please refer to Figure S4. The random distribution of the pyramids with its (111) facets is clearly apparent in Figure 1c. The typical size of these pyramids is in the range of 1- 12 µm. We compared different etch times in opto-electrical regime to determine the highest performing pyramid structure as shown in Fig. S1 and Fig. S2. We note that longer etch time improves performance until the entire surface is filled with pyramids of different sizes.
It is important to emphasize that each structure was independently optimised for etch depth and fill factor and we determine the etch depth of the highest performing QR to be (80 ± 10) nm. For the pyramids, their bases range up to 1500 nm in size as shown in Figure 2d. The performances as a function of etch depth for the different structures are shown in Figs. S2- S4.

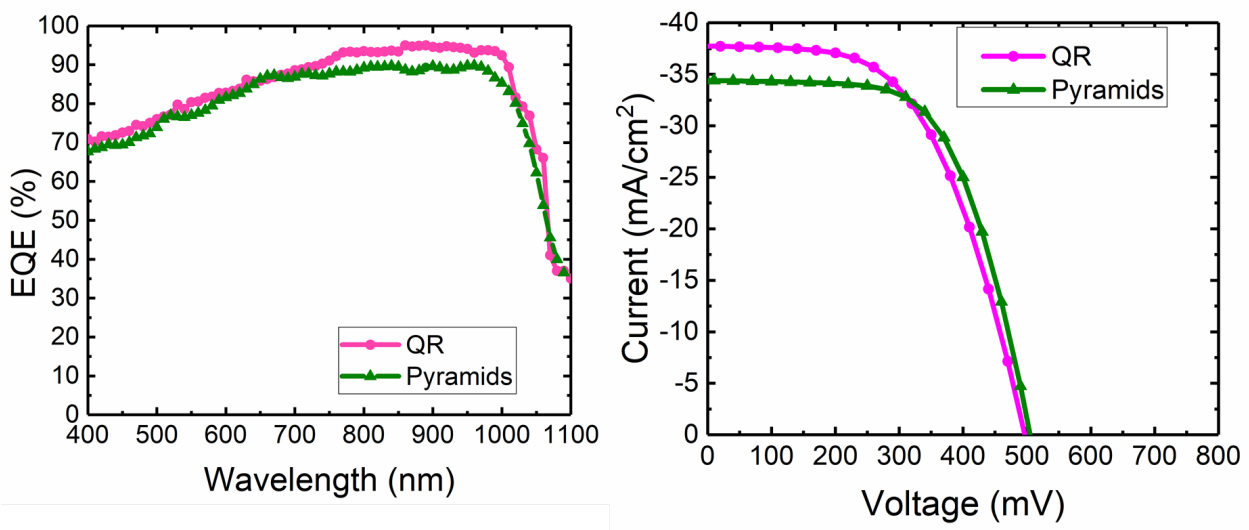


**Figure 3.** Comparison of a) the external quantum efficiency of the two structures over the wavelength range from 400 to 1100 nm and b) Comparison of the I-V curves of pyramids vs the QR structures.

Finally, we assessed the electrical impact of the surface structure via the external quantum efficiency (EQE) and the I-V curves of the finished devices, shown in Figure 3. While the differences are subtle, we note (fig. 3b) that the QR outperforms the pyramids overall by generating a higher short circuit current. This is surprising given the higher overall absorption of the pyramids we noted in figs. 1b/c. Indeed, we also note from the EQE that the pyramids perform slightly better at longer wavelength, i.e. above 1000 nm. As the wavelength gets shorter, however, this trend is reversed and the QR exhibits a higher EQE, even at very short wavelength where the absorption of the QR drops again. This higher EQE of the QR combined with lower absorption in the blue is indicative of lower surface charge recombination: at shorter wavelength, light is increasingly absorbed near the front surface. Consequently, surface charge recombination becomes predominant and is more severe in the pyramids, due to their larger surface area. That's why the pyramids, despite their slightly better absorption properties, overall perform less well than the QR. This result indicates that binary nanostructures such as the QR can be advantageous over pyramids even in the domain of thicker solar cells, due to a favourable trade-off between absorption and surface charge recombination. The main parameters are summarized in Table S1.

The curves shown here are representative of a large number of samples and we typically observe deviations of less than ±5 mV between nominally identical samples made in different batches.

While we do not claim that we are comparing the very best pyramidal structure, we still find it remarkable that the QR structure, which was originally designed for thin film silicon devices, also performs well in bulk solar cells, and better than the widely used random pyramids. These results indicate that the high optical performance of binary nanostructures, combined with their potential to reduce surface recombination, might be a solution to improve the performance even in thick silicon solar cells. Naturally, such a result would need to be confirmed with the high-efficiency cells referred to in the introduction, and it would need to be tensioned against the increased cost of applying nanostructures, e.g. by roll-to-roll printing techniques, nevertheless it is intriguing that this opportunity now exists.

To summarise, we have shown that solar cells patterned with deterministic, quasirandom binary nanostructures have larger $J_{sc}$ than randomly etched pyramidal structures. We identified that the larger $J_{sc}$ results from a favourable trade-off between absorption and charge carrier recombination. In more detail, we can also answer the two questions posed in the introduction, namely, 1 – is the optical performance of binary nanostructures comparable to that of pyramids, especially in thick solar cells? The optical performance of pyramids is overall better because it is more broadband and because it affords better light trapping at the long wavelengths above 1000 nm. 2 – is the electrical performance of binary nanostructures better or worse than that of pyramids? Binary nanostructures such as the QR structure studied here have better electrical properties because of their lower surface area.

The overall improvement is somewhat unexpected, as the quasirandom class of structures was invented to improve light trapping in thin film solar cells, but not in thick devices. We further speculate that their very good optical performance in the 600-800 nm wavelength range, where they offer comparable performance to high aspect ratio pyramids (HARPs), relates to the controlled number of diffraction channels offered by the quasirandom approach. This controlled number of channels is designed to favour diffraction into guided modes with high absorptivity rather than random scattering [22], thereby minimising the excitation of air modes, i.e. reflection.

In conclusion, we have compared different nanostructures on real solar cell devices and demonstrated that we can obtain a short circuit current as high as 38 mA/cm$^2$ with dry etched structures, which is close to the State-of-the-Art for silicon and which demonstrates that quasirandom nanostructures have an important role to play even in bulk silicon devices.

**Supporting Information**. Supporting Information is available free of charge from the IEEE Photonics home page. Nano-structures fabrication for different etch-depth parameter, Further characterization comparison of fabricated devices, design details of quaisrandom structures. (PDF)

ACKNOWLEDGMENT

TFK acknowledges support through a Royal Society Wolfson Merit Award. AS gratefully acknowledges PhD studentship awarded by National University of Sciences and Technology under “Faculty Development programme (FDP) 2014”, Islamabad, Pakistan.

REFERENCES

[1] L. Guilin, Wang Jianqiang, Q. Zhengyi, and W. Shen, “Development of back-junction back-contact silicon solar cells based on industrial processes,” *Prog*, vol. 25, pp. 441–451, 2017.

[2] M. A. Green, K. Emery, Y. Hishikawa, W. Warta, and E. D. Dunlop, “Solar cell efficiency

tables (version 46)," *Prog. Photovoltaics Res. Appl.*, vol. 23, pp. 805–812, 2015.

[3] M. A. Green, Y. Hishikawa, W. Warta, E. D. Dunlop, D. H. Levi, J. Hohl-Ebinger, and A. W. H. Ho-Baillie, "Solar cell efficiency tables (version 50)," *Prog. Photovoltaics Res. Appl.*, vol. 25, no. 7, pp. 668–676, 2017.

[4] A. Polman, M. Knight, E. C. Garnett, B. Ehrler, and W. C. Sinke, "Photovoltaic materials: Present efficiencies and future challenges.," *Science (New York, N.Y.)*, vol. 352, no. 6283, pp. 307–311, 2016.

[5] J. Zhao, A. Wang, M. A. Green, and F. Ferrazza, "19.8% Efficient 'Honeycomb' Textured Multicrystalline and 24.4% Monocrystalline Silicon Solar Cells," *Appl. Phys. Lett.*, vol. 73, no. 14, pp. 1991–1993, 1998.

[6] P. Yu, J. Wu, S. Liu, J. Xiong, C. Jagadish, and Z. M. Wang, "Design and fabrication of silicon nanowires towards efficient solar cells," *Nano Today*, vol. 11, no. 6, pp. 704–737, 2016.

[7] A. Gaucher, A. Cattoni, C. Dupuis, W. Chen, R. Cariou, M. Foldyna, L. Lalouat, E. Drouard, C. Seassal, P. Roca i Cabarrocas, and S. Collin, "Ultrathin Epitaxial Silicon Solar Cells with Inverted Nanopyramid Arrays for Efficient Light Trapping," *Nano Lett.*, vol. 16, no. 9, pp. 5358–5364, Sep. 2016.

[8] E. R. Martins, J. Li, Y. Liu, J. Zhou, and T. F. Krauss, "Engineering gratings for light trapping in photovoltaics: The supercell concept," *Phys. Rev. B - Condens. Matter Mater. Phys.*, vol. 86, no. 4, pp. 1–4, 2012.

[9] K. X. Wang, Z. Yu, V. Liu, Y. Cui, and S. Fan, "Absorption enhancement in ultrathin crystalline silicon solar cells with antireflection and light-trapping nanocone gratings," *Nano Lett.*, vol. 12, no. 3, pp. 1616–1619, 2012.

[10] Q. Lin, S. F. Leung, L. Lu, X. Chen, Z. Chen, H. Tang, W. Su, D. Li, and Z. Fan, "Inverted nanocone-based thin film photovoltaics with omnidirectionally enhanced performance," *ACS Nano*, vol. 8, pp. 6484–6490, 2014.

[11] S.-F. Leung, K.-H. Tsui, Q. Lin, H. Huang, L. Lu, J.-M. Shieh, C.-H. Shen, C.-H. Hsu, Q. Zhang, D. Li, and Z. Fan, "Large scale, flexible and three-dimensional quasi-ordered aluminum nanospikes for thin film photovoltaics with omnidirectional light trapping and optimized electrical design," *Energy Environ. Sci.*, vol. 7, pp. 3611–3616, 2014.

[12] H. Sai, Y. Kanamori, K. Arafune, Y. Ohshita, and M. Yamaguchi, "Light trapping effect of submicron surface textures in crystalline Si solar cells," *Prog. Photovoltaics Res. Appl.*, vol. 15, no. 5, pp. 415–423, Aug. 2007.

[13] M. F. Abdullah, M. A. Alghoul, H. Naser, N. Asim, S. Ahmadi, B. Yatim, and K. Sopian, "Research and development efforts on texturization to reduce the optical losses at front surface of silicon solar cell," *Renew. Sustain. Energy Rev.*, vol. 66, pp. 380–398, 2016.

[14] F. Llopis and I. Tobías, "Influence of texture feature size on the optical performance of silicon solar cells," *Prog. Photovoltaics Res. Appl.*, vol. 13, pp. 27–36, 2005.

[15] J. Zhu, C.-M. Hsu, Z. Yu, S. Fan, and Y. Cui, "Nanodome solar cells with efficient light management and self-cleaning.," *Nano Lett.*, vol. 10, pp. 1979–84, Jun. 2010.

[16] K. Peng, S. Lee, H. Kong, and A. C. Society, "High Performance Silicon Nanohole Solar Cells," *J. Am. Chem. Soc.*, vol. 132, pp. 6872–6873, 2010.

[17] X. Liu, P. R. Coxon, M. Peters, B. Hoex, J. M. Cole, and D. J. Fray, "Black silicon: fabrication methods, properties and solar energy applications," *Energy Environ. Sci.*, vol. 7, pp. 3223–3263, 2014.

[18] J. Oh, H. C. Yuan, and H. M. Branz, "An 18.2% efficient black-silicon solar cell achieved through control of carrier recombination in nanostructures," *Nat. Nanotechnol.*, vol. 7, pp. 743–748, 2012.

[19] H. Savin, P. Repo, G. von Gastrow, P. Ortega, E. Calle, M. Garín, and R. Alcubilla, "Black silicon solar cells with interdigitated back-contacts achieve 22.1% efficiency.," *Nat. Nanotechnol.*, vol. 10, pp. 1–6, 2015.

[20] M. . Green, K. Emery, Y. Hishikawa, W. Warta, and E. D. Dunlop, "Solar cell efficiency tables (version 43)," *Prog. Photovolt Res. Appl.*, vol. 22, pp. 1–9, 2014.

[21] M. A. Green, K. Emery, Y. Hishikawa, W. Warta, and E. D. Dunlop, "Solar cell efficiency tables (Version 45)," *Prog. Photovolt Res. Appl.*, vol. 23, pp. 1–9, 2015.

[22] J. Li, K. Li, C. Schuster, R. Su, X. Wang, B. H. V Borges, T. F. Krauss, and E. R. Martins, "Spatial resolution effect of light coupling structures," *Sci. Rep.*, vol. 5, pp. 1–8, 2015.

[23] K. Li, J. Li, C. Reardon, C. S. Schuster, Y. Wang, G. J. Triggs, N. Damnik, J. Muënchenberger, X. Wang, E. R. Martins, and T. F. Krauss, "High speed e-beam writing for large area photonic nanostructures-a choice of parameters," *Sci. Rep.*, vol. 6, pp. 1–10, 2016.

[24] M. S. Branham, W.-C. Hsu, S. Yerci, J. Loomis, S. V Boriskina, B. R. Hoard, S. E. Han, A. Ebong, and G. Chen, "Empirical Comparison of Random and Periodic Surface Light-Trapping Structures for Ultrathin Silicon Photovoltaics," *Adv. Opt. Mater.*, vol. 4, no. 6, pp. 858–863, Mar. 2016.

[25] D. M. Whittaker and I. S. Culshaw, "Scattering-matrix treatment of patterned multilayer photonic structures," *Phys. Rev. B*, vol. 60, no. 4, pp. 2610–2618, 1999.

[26] Y. Da and Y. Xuan, "Role of surface recombination in affecting the efficiency of nanostructured thin-film solar cells.," *Opt. Express*, vol. 21 Suppl 6, pp. A1065-77, Nov. 2013.

[27] J. Oh, H.-C. Yuan, and H. M. Branz, "An 18.2%-efficient black-silicon solar cell achieved through control of carrier recombination in nanostructures," *Nat. Nanotechnol.*, vol. 7, p. 743, Sep. 2012.

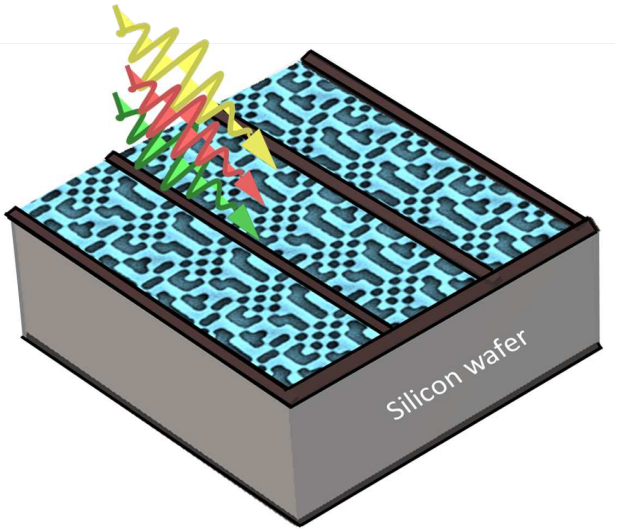


For Table of Contents Only